Mixed-Oxide Catalysts | Hot Paper

DOI: 10.1002/ange.201402435

Stabilization of Catalytically Active Cu^+ Surface Sites on Titanium–Copper Mixed-Oxide Films**

*Ashleigh E. Baber, Xiaofang Yang, Hyun You Kim, Kumudu Mudiyanselage, Markus Soldemo, Jonas Weissenrieder, Sanjaya D. Senanayake, Abdullah Al-Mahboob, Jerzy T. Sadowski, Jaime Evans, José A. Rodriguez, Ping Liu, Friedrich M. Hoffmann, Jingguang G. Chen, and Darío J. Stacchiola**

Abstract: *The oxidation of CO is the archetypal heterogeneous catalytic reaction and plays a central role in the advancement of fundamental studies, the control of automobile emissions, and industrial oxidation reactions. Copper-based catalysts were the first catalysts that were reported to enable the oxidation of CO at room temperature, but a lack of stability at the elevated reaction temperatures that are used in automobile catalytic converters, in particular the loss of the most reactive Cu^+ cations, leads to their deactivation. Using a combined experimental and theoretical approach, it is shown how the incorporation of titanium cations in a Cu_2O film leads to the formation of a stable mixed-metal oxide with a Cu^+ terminated surface that is highly active for CO oxidation.*

The natural abundance of cuprous oxide (Cu_2O) and its optimal catalytic properties for reactions ranging from CO oxidation[1] to photocatalytic water splitting[2] have made it a prime target for catalyst research. Although the controlled synthesis of nanoscale cuprous oxide particles is being actively pursued to optimize its properties,[3] the Achilles heel of Cu_2O catalysts has been their deactivation by complete oxidation to CuO[4] or by reduction to Cu^0;[5] both processes lead to the loss of the catalytically active Cu^+ centers.[6] The first catalyst that was reported to oxidize CO at room temperature was hopcalite, a copper–manganese mixed oxide, which was described in the early twentieth century. The full oxidation of Cu^+ to Cu^{2+} cations at higher temperatures led to a significant decrease in its activity when used in hot automobile catalytic converters,[4] and its activity was further reduced by deactivation processes that are due to sulfur and water. Therefore, expensive noble metals have been used for practical oxidation methods since the 1970s.[1] The high cost of noble metals and the decrease in the sulfur content of gasoline have contributed to the renewed interest in inexpensive oxidation catalysts, among which cobalt- and copper-based catalysts are the only two that are expected to succeed.[1,7] Herein, we demonstrate how the controlled addition of titanium to a Cu_2O surface leads to the formation of a titanium–copper mixed-oxide film that exposes thermally and chemically stabilized Cu^+ sites, which improves the already high activity of the Cu_2O catalysts towards CO oxidation.

A well-ordered $Cu_2O(111)$ row structure can be formed by oxidizing Cu(111) (Supporting Information, Figure S1).[5,8] The deposition of titanium onto a $Cu_2O(111)$ film at 300 K leads to the formation of small TiO_x clusters and partial reduction of the film. Annealing this TiO_x–CuO_x system in oxygen to 650 K leads to the formation of the surface that is shown in Figure 1 A, which was imaged by scanning tunneling microscopy (STM); the formation of hexagonal islands and modified Cu_2O terraces was thus revealed. Hexagonal islands grow in the vicinity of step edges and increase in size and density as a function of the titanium coverage.

The low-energy electron diffraction (LEED) pattern that is obtained after depositing 0.7 monolayers (ML) of Ti onto the Cu_2O film is shown in Figure 1 B (for LEED patterns that show the evolution from Cu(111) to the $TiCuO_x$ film, see Figure S2). The pattern corresponds to a hexagonally packed

[*] Dr. A. E. Baber, Dr. X. Yang, Dr. K. Mudiyanselage, Dr. S. D. Senanayake, Dr. J. A. Rodriguez, Dr. J. G. Chen, Dr. D. J. Stacchiola
Chemistry Department, Brookhaven National Laboratory (BNL)
Upton, NY 11973 (USA)
E-mail: djs@bnl.gov

M. Soldemo, Dr. J. Weissenrieder
KTH Royal Institute of Technology, Material Physics
Stockholm (Sweden)

Dr. H. Y. Kim,[+] Dr. A. Al-Mahboob, Dr. J. T. Sadowski, Dr. P. Liu
Center for Functional Nanomaterials (CFN), BNL (USA)

Dr. J. Evans
Facultad de Ciencias, Universidad Central de Venezuela
Caracas 1020A (Venezuela)

Dr. F. M. Hoffmann
Department of Science, BMCC-CUNY
New York, NY 10007 (USA)

Dr. J. G. Chen
Department of Chemical Engineering, Columbia University
New York, NY 10027 (USA)

[+] Current address: Department of Nanomaterials Engineering
Chungnam National University, 99 Daehak-ro
Yuseong-gu, Daejeon 305-764, (Korea)

[**] Work carried out at BNL was supported by the US DOE, Office of BES (DE-AC02-98CH10086). Calculations were performed at the CFN. We are thankful to the Swedish Research Council (VR) for financial support. Jan Knudsen, Joachim Schnadt, and the Max-lab staff are acknowledged for their support.

Supporting information for this article is available on the WWW under http://dx.doi.org/10.1002/anie.201402435.

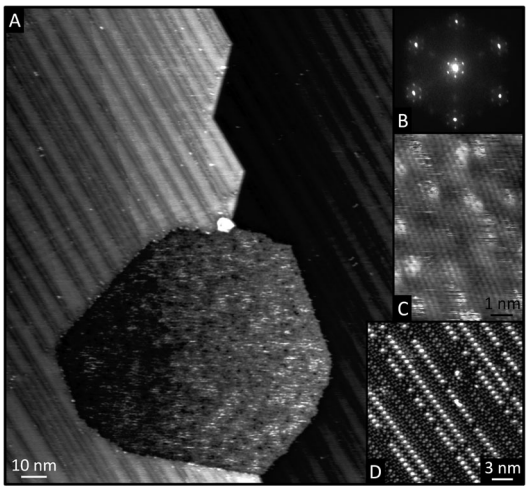

Figure 1. STM images and LEED pattern of a $TiCuO_x$ film (ca. 0.5 ML Ti). A) Large-scale STM image of hexagonal islands and row-structured terraces (STM: −0.16 V, 0.21 nA). B) A hexagonal Moiré pattern is obtained by LEED (ca. 0.7 ML Ti coverage). C) Atomically resolved hexagonal island, observed by STM (0.03 V, 1.30 nA). D) High-resolution STM image of the titanium-modified Cu_2O terrace (−0.50 V, 0.27 nA).

surface with Moiré spots. Hexagonal (1×1) Cu(111) substrate spots are observed the farthest from the center spot (spacing: 0.256 nm). The addition of Ti leads to intense spots that correspond to a spacing of 0.295 ± 0.001 nm and Moiré spots around the zero point (1.66 ± 0.04 nm). An atomically resolved STM image of a hexagonal island (Figure 1C) exhibits a Moiré structure (1.82 ± 0.15 nm) as well as a close-packed hexagonal structure (0.28 ± 0.02 nm), which is in line with the LEED measurements (Figure 1B). The terraces that are shown in Figure 1A preserve the underlying row structure of the $Cu_2O(111)$ film, but also contain brighter rows across the surface. A high-resolution image of a terrace reveals a well ordered structure with bright protrusions along the rows (Figure 1D). The density of the bright protrusions correlates with the titanium coverage. The increase in the densities of the hexagonal islands and modified Cu_2O terraces upon an increase in titanium coverage indicates that both structures are related to the presence of titanium.

Near-edge X-ray absorption fine structure (NEXAFS) measurements were performed to determine the location and electronic structure of the titanium atoms in the $TiCuO_x$ film. The top panel of Figure 2 presents Ti L-edge spectra of the $TiCuO_x$ surfaces. The four peaks in each spectrum correspond to the electronic transitions from the occupied spin–orbit-split 2p states, L_2 and L_3, to the unoccupied crystal-field-split d states, t_{2g} and e_g.[9] In the O K-edge spectra for the same systems, two sharp peaks are observed at 531.1 and 534.0 eV; these peaks correspond to the transition of O 1s core electrons to the empty 2p-hybridized states t_{2g} and e_g (Figure 2, bottom). The fine structure of the Ti L_3-e_g peak is strongly correlated with the TiO_6 octahedral structure, the building block of TiO_2, and has been used as a fingerprint to identify the two most stable phases of TiO_2, rutile and anatase. The TiO_6 octahedra in both the rutile and anatase phases are distorted and connected to each other through edges or

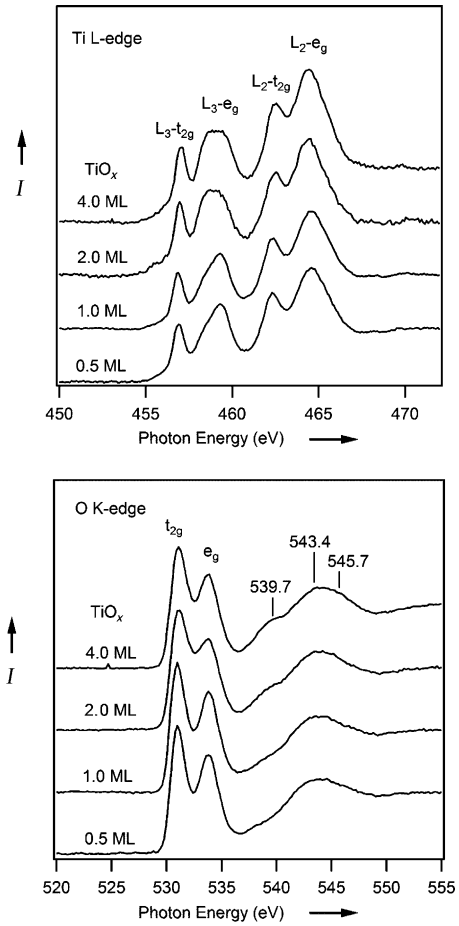

Figure 2. NEXAFS spectra of $TiCuO_x$ films.

corners. However, recent studies suggest that the line shape of the L_3-e_g peak is mainly determined by long-range bonding properties rather than by the local structure of the TiO_6 unit.[10]

Non-local structures cause multiple scattering scenarios during X-ray absorption, which results in different splittings of the L_3-e_g peak. In this study, the L_3-e_g peaks of $TiCuO_x$ clearly vary with titanium coverage. At low coverages, the L_3-e_g peaks are characterized by a single asymmetric feature at 459.3 eV, which does not fully match the fingerprint of either the rutile or the anatase phase. As the coverage of TiO_x increases to 2.0 and 4.0 ML, the splitting becomes clear for two of the L_3-e_g peaks, indicating the transition from a mixed oxide to a bulk-like titania film. A similar trend was observed in the O K-edge spectra. As the coverage reached 2.0 ML, a new peak appeared at 539.7 eV, and the three broad peaks in the high-energy region are in good agreement with the O K-edge spectra of bulk titania.[9] For various titanate mixed oxides, such as $ScTiO_3$ and CeO_2–TiO_2,[11] the spectra do not show splitting of the L_3-e_g peaks. Therefore, it may be assumed that a mixed $TiCuO_x$ oxide layer is formed at titanium coverages below 1.0 ML.

CO adsorption was used to probe the exposed surface sites on the $TiCuO_x$ film with submonolayer coverages of titanium. Figure 3 shows the infrared reflection absorption

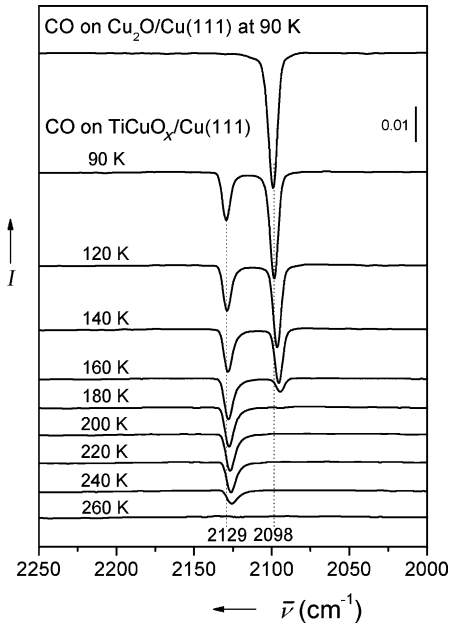

Figure 3. IRRAS spectra of CO adsorption on a $TiCuO_x$ film from 90 K to 260 K. CO adsorption on a Cu_2O film is displayed for comparison (top).

spectroscopy (IRRAS) data that was obtained after the saturated adsorption of CO on $TiCuO_x$ at 90 K: Two peaks appeared at 2098 and 2129 cm^{-1}. The peak at 2098 cm^{-1} can be assigned to CO that is adsorbed onto Cu^+ cations of pure Cu_2O,[12] and this peak decreases in intensity with an increase in the amount of titanium (not shown). The reduced intensity of the peak at 2098 cm^{-1} for the $TiCuO_x$ films with respect to the intensity for the Cu_2O film can be used to estimate the coverage of pure Cu_2O. Approximately 75% of the $TiCuO_x$ surface shown in Figure 3 is covered with pure Cu_2O. CO adsorption on the Ti^{4+} sites of rutile $TiO_2(110)$ leads to a peak at 2188 cm^{-1}.[13] It is unlikely that the IR peak for adsorbed CO on Ti^{4+} could red-shift to 2129 cm^{-1} from its value of 2188 cm^{-1} for rutile TiO_2. Therefore, the peak at 2129 cm^{-1} correlates more closely with that for CO molecules that are adsorbed on Cu^+ sites and perturbed by the presence of titanium, rather than with CO molecules that are adsorbed on Ti ions in the presence of copper atoms. Furthermore, a small feature at 2163 cm^{-1} is observed for high coverages of Ti on the $TiCuO_x$ film (not shown), indicating a shift to higher wavenumbers and a more bulk-like titania, which is not the case for low coverages of Ti. The peak for adsorbed CO on top of a partially reduced Ti cation near the oxygen vacancies of reduced rutile $TiO_2(110)$ is observed at 2178 cm^{-1}.[13] When the $TiCuO_x$ sample was annealed, the intensity of the peak at 2098 cm^{-1} for CO on Cu^+ of pure Cu_2O regions gradually decreased and completely disappeared at a temperature of 180 K, which is in agreement with the behavior that was observed for CO adsorbed on Cu_2O films.[12] The intensity of the peak at 2129 cm^{-1} remains unchanged until much higher temperatures and disappears completely by 260 K. CO desorbs completely from rutile $TiO_2(110)$ at 150 K,[14] and from the Cu_2O film or Cu(111) at 180 K.[12] Therefore, the data in Figure 3 clearly show that CO adsorbs more strongly on $TiCuO_x$ than on either rutile $TiO_2(110)$ or Cu_2O films. When the coverage of Ti is increased, STM indicates an increase in the density of the large hexagonal islands shown in Figure 1, and IRRAS shows that the adsorption of CO on any Cu^+ sites is completely suppressed. Overall, these observations indicate that the stable adsorption site for CO is not on the hexagonal islands, but rather on the terraces that are shown in Figure 1D, where a titanium-modified Cu_2O row structure is observed.

To model the titanium-modified Cu_2O row structure that was observed on the terraces of the $TiCuO_x$ film by STM (Figure 1D and Figure 4B), DFT calculations were performed utilizing the structural motif of well-defined mono-

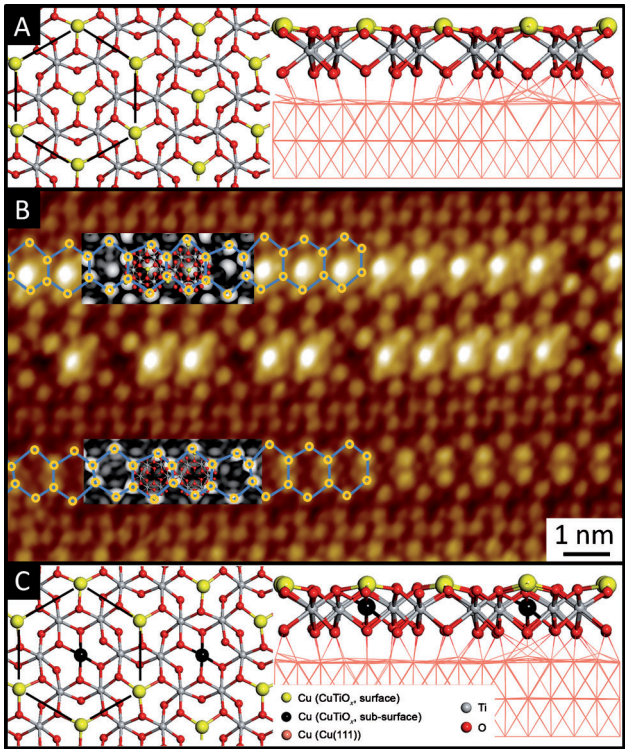

Figure 4. A–C) Comparison of the structures predicted by DFT calculations with an STM image of the $TiCuO_x$ terraces. A) All Cu atoms at the surface layer. B) DFT structures and simulated images superimposed on an STM image (−0.50 V, 0.27 nA. C) Central copper atoms (black) in the subsurface of the film.

clinic Li_2TiO_3. The lithium ions of Li_2TiO_3 were replaced with Cu and fully optimized, which resulted in the formation of two types of Cu sites: The first site is located at the same position as the titanium atoms in the O–TiCu–O trilayer; the second site interconnects the two trilayers (Figure S3). A single O–TiCu–O trilayer with coordinating oxygen atoms was sliced and optimized on the Cu(111) substrate. A 7×7 Cu(111) substrate was chosen to minimize the lattice mismatch with the Cu_2TiO_3 layer (Figure S3). The two structures for the $TiCuO_x$ films that were predicted by DFT calculations are presented in Figure 4. Most of the copper atoms that were originally located in the same plane as the titanium ions

relocate to the surface layer to form a hexagonal copper framework (Figure 4A), with a local oxygen coordination number (CN) of three; the copper atoms are separated by 0.9 nm. The CN of three is unique for a copper oxide structure, as Cu_2O and CuO have CNs of 2 and 4, respectively, and Cu_3O_4 a mixture of 2 and 4. The long distance between the surface Cu^+ cations in the mixed oxide inhibits the facile dissociation of adsorbed oxygen molecules, which prevents further oxidation to Cu^{2+}. Preliminary calculations indicate that dissociation of oxygen can easily occur at the step edges of the mixed-oxide film. All of the titanium atoms in the mixed-oxide film remain isolated and in the subsurface region of the film, which is in agreement with the results that were obtained from NEXAFS and IRRAS and described above. With a relatively small energy barrier of 0.23 eV nm^{-2} or 0.35 eV nm^{-2}, half or all of the central copper atoms (●, Figure 4C) can be pulled back to the subsurface layer forming periodic hexagonal rows at the surface layer (Figure 4B).

Simulated filled-state STM images of these two structures that were predicted by DFT calculations confirm that the bright spots in the experimental STM images may be due to copper atoms in the surface layer. The distance between two adjacent subsurface copper atoms in the DFT model (●, Figure 4C) was found to be 0.894 nm, reproducing the experimental value of 0.89 ± 0.01 nm between the hexagons along a row. Figures 4A and 4C show that the number of Cu–O interatomic bonds between the bottom layer of oxygen atoms in $TiCuO_x$ and the first layer of the Cu(111) substrate depends on the location of the central copper atoms in the copper hexagons. The number of bonds between the $TiCuO_x$ film and Cu(111) is reduced when the central copper atoms of the hexagons are located in the subsurface of the film, thus weakening the interaction between the substrate and the film. As a result, the strain generated at the interface between the surface layer and the Cu(111) substrate, which would be present in films in which all of the copper atoms are located in the surface layer (Figure 4A), is reduced. Experimentally, a combination of both structures is observed, which helps to release strain at the Cu(111) substrate.

The $TiCuO_x$ mixed-oxide films showed activity for CO oxidation at room temperature. Their stability and catalytic activity for CO oxidation were compared with the results that were obtained with clean Cu_2O films at temperatures that are commonly found in catalytic converters. An Arrhenius plot for the CO oxidation is shown in Figure 5. The CO_2 production rate is significantly improved by the addition of titanium to the Cu_2O film. More importantly, the formation of the mixed oxide helps to stabilize the active sites on the surface of the catalyst. For the Cu_2O film, its catalytic activity drops to half of its original value in two hours during CO oxidation, whereas for the $TiCuO_x$ film, there is only a very small initial drop in activity (Figure 5, inset).

The chemical state of the oxide films during CO oxidation was interrogated by in situ ambient-pressure X-ray photoelectron spectroscopy (AP-XPS). Figure 6 shows the O 1s regions of both $TiCuO_x$ and Cu_2O films during CO oxidation at 300 K. The spectra were taken at a low conversion into CO_2, approximately ten minutes after the start of the reaction. The peak at 530.0 eV corresponds to oxygen from the original

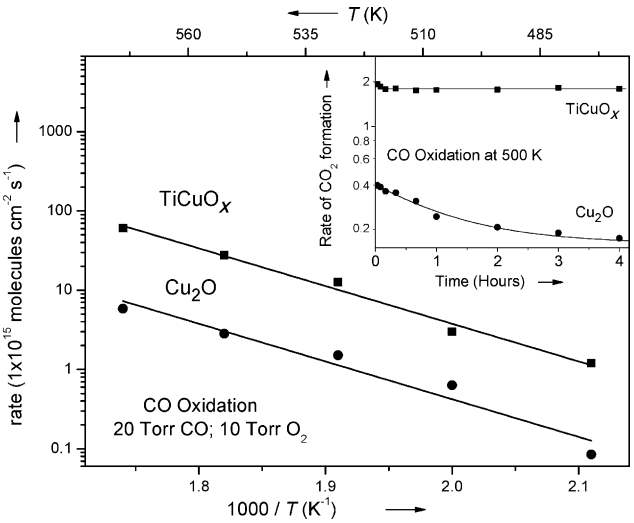

Figure 5. Arrhenius plot of the CO oxidation on Cu_2O and $TiCuO_x$ (ca. 0.6 ML Ti) films. Inset: Catalyst stability during a reaction at 500 K.

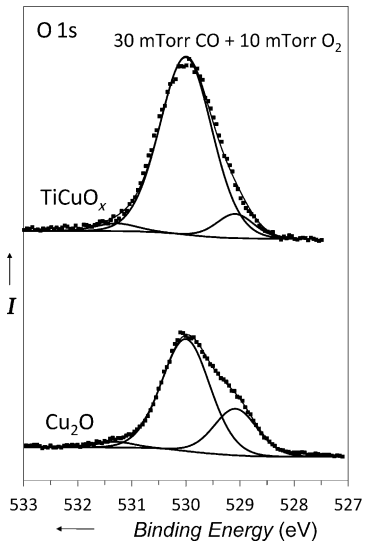

Figure 6. In situ AP-XPS of $TiCuO_x$ (ca. 0.5 ML Ti) and Cu_2O/Cu(111) films during the oxidation of CO at 300 K.

oxide films. Under an environment of CO and O_2 at elevated pressures, two new peaks develop: one peak at 531.2 eV, which is related to the formation of a small amount of hydroxy groups[15] because of an increase in the amount of background water, and a second peak at 529.1 eV, which is due to the formation of CuO.[16] The $TiCuO_x$ film with a submonolayer load of Ti (0.5 ± 0.1 ML) gives only a small CuO peak (529.1 eV), which is likely associated with regions of pure Cu_2O, compared to the larger peak that was observed for the Cu_2O film. The presence of titanium preserves the highly active Cu^+ sites on the surface and thus prevents deactivation of the catalysts. At the higher reaction temperatures encountered in catalytic converters (Figure 5), the oxidation of Cu_2O is more pronounced, and the protection of the $TiCuO_x$ becomes critical, as shown by the stability data in the inset of Figure 5. To further test the enhanced stability of

the $TiCuO_x$ surface, the films were exposed to CO. Exposure of the Cu_2O film to 1 Torr of CO resulted in full reduction of the film,[5] but $TiCuO_x$ films treated under the same conditions remained intact. The same observations were made when the films were exposed to a mixture of CO and water.

Historically, the complexity and lack of stability of mixed copper oxide materials under the commonly used reaction conditions have prevented their widespread use, even though their low cost and physicochemical properties render them promising catalysts for CO oxidation.[1] We have synthesized stable $TiCuO_x$ films that are very active in CO oxidation, and by combining microscopic and spectroscopic experimental studies with theoretical simulations, we have been able to describe their complex structure at the atomic level. The presence of titanium prevents the oxidation and reduction of the Cu_2O films under the reaction conditions, thereby enhancing the robustness of the catalyst. Furthermore, the presence of titanium stabilizes the Cu^+ ions on the surface that are locally coordinated to three oxygen atoms, and that act as better adsorption sites for CO than sites on pure TiO_2 or Cu_2O. This finding and the description of its origin can help to develop efficient copper-based oxidation catalysts.

Experimental Section

IRRAS was performed in a UHV-Reactor cell system.[17] An Omicron STM was used to image films. LEED and NEXAFS were obtained in NSLS, at beamlines U5UA and U12a. AP-XPS was conducted in the Maxlab at Lund University (Sweden), at beamline I511-1.[18] Spin-polarized DFT calculations were performed with a plane-wave basis. Further details are provided in the Supporting Information.

Received: February 14, 2014
Published online: April 9, 2014

Keywords: CO oxidation · IR spectroscopy · mixed oxides · scanning tunneling microscopy · surface chemistry

[1] S. Royer, D. Duprez, *ChemCatChem* **2011**, *3*, 24 – 65.
[2] A. Paracchino, V. Laporte, K. Sivula, M. Gratzel, E. Thimsen, *Nat. Mater.* **2011**, *10*, 456 – 461.
[3] W. Huang, L. Lyu, Y. Yang, M. Huang, *J. Am. Chem. Soc.* **2012**, *134*, 1261 – 1267.
[4] G. G. Jernigan, G. A. Somorjai, *J. Catal.* **1994**, *147*, 567 – 577.
[5] A. Baber, F. Xu, F. Dvorak, K. Mudiyanselage, M. Soldemo, J. Weissenrieder, S. Senanayake, J. Sadowski, J. Rodriguez, V. Matolin, M. White, D. Stacchiola, *J. Am. Chem. Soc.* **2013**, *135*, 16781 – 16784.
[6] T. J. Huang, D. H. Tsai, *Catal. Lett.* **2003**, *87*, 173 – 178.
[7] X. W. Xie, Y. Li, Z. Q. Liu, M. Haruta, W. J. Shen, *Nature* **2009**, *458*, 746 – 749.
[8] a) F. Yang, Y. Choi, P. Liu, D. Stacchiola, J. Hrbek, J. A. Rodriguez, *J. Am. Chem. Soc.* **2011**, *133*, 11474 – 11477; b) F. Jensen, F. Besenbacher, E. Laegsgaard, I. Stensgaard, *Surf. Sci.* **1991**, *259*, L774 – L780.
[9] J. G. Chen, *Surf. Sci. Rep.* **1997**, *30*, 1 – 152.
[10] P. Guttmann, C. Bittencourt, S. Rehbein, P. Umek, X. X. Ke, G. Van Tendeloo, C. P. Ewels, G. Schneider, *Nat. Photonics* **2011**, *6*, 25 – 29.
[11] a) P. Krüger, *Phys. Rev. B* **2010**, *81*, 125121; b) S. Kundu, J. Ciston, S. D. Senanayake, D. A. Arena, E. Fujita, D. Stacchiola, L. Barrio, R. M. Navarro, J. L. G. Fierro, J. A. Rodriguez, *J. Phys. Chem. C* **2012**, *116*, 14062 – 14070.
[12] K. Mudiyanselage, W. An, F. Yang, P. Liu, D. J. Stacchiola, *Phys. Chem. Chem. Phys.* **2013**, *15*, 10726 – 10731.
[13] M. C. Xu, H. Noei, K. Fink, M. Muhler, Y. M. Wang, C. Woll, *Angew. Chem.* **2012**, *124*, 4810 – 4813; *Angew. Chem. Int. Ed.* **2012**, *51*, 4731 – 4734.
[14] N. G. Petrik, G. A. Kimmel, *J. Phys. Chem. Lett.* **2012**, *3*, 3425 – 3430.
[15] D. F. Ogletree, H. Bluhm, E. D. Hebenstreit, M. Salmeron, *Nucl. Instrum. Methods Phys. Res. Sect. A* **2009**, *601*, 151 – 160.
[16] P. Jiang, D. Prendergast, F. Borondics, S. Porsgaard, L. Giovanetti, E. Pach, J. Newberg, H. Bluhm, F. Besenbacher, M. Salmeron, *J. Chem. Phys.* **2013**, *138*, 024704.
[17] J. Hrbek, F. M. Hoffmann, J. B. Park, P. Liu, D. Stacchiola, Y. S. Hoo, S. Ma, A. Nambu, J. A. Rodriguez, M. G. White, *J. Am. Chem. Soc.* **2008**, *130*, 17272 – 17273.
[18] J. Schnadt, J. Knudsen, J. N. Andersen, H. Siegbahn, A. Pietzsch, F. Hennies, N. Johansson, N. Martensson, G. Ohrwall, S. Bahr, S. Mahl, O. Schaff, *J. Synchrotron Radiat.* **2012**, *19*, 701 – 704.

